

# Particle Holography and the noise limit

S.F. Herrmann and K.D. Hinsch

**Abstract** In particle holography the available amount of laser energy limits the size of the region under investigation. This especially holds in holographic PIV (HPIV) where tiny tracer particles are used to probe air flows. To achieve maximum diffraction efficiency the recording of a hologram on silver-halide film requires typically an object-to-reference intensity ratio of  $r = 0.25$ . At the expense of image intensity this ratio can be decreased by several orders of magnitude depending on the type of object and the scattering behavior of the granular structures in the film emulsion. With less object light needed for recording, larger measuring volumes become feasible for a variety of new applications. However, during reconstruction a long time exposure must be provided for the extraction of particle images. General experiments have been carried out to find the noise limit for proper registration of objects with varying spatial frequencies and model particle fields. Concluding, a theory based on a checkerboard model of scatterers provides a good prediction of tendencies observed in the experiment.

## 1

### Particle Holography and PIV

Particle image velocimetry (PIV), an originally planar technique to measure velocities, was extended by particle holography since the high resolution and excellent reconstruction fidelity of holograms permit measurements in three-dimensional space.

Successful experimental realizations of HPIV have all be concerned with noise problems due to a superimposed speckle field originating from a variety of sources. Noise suppression can be achieved using low coherence light sources and localizing depth information at specific regions of the holographic plate, a principle recently introduced in HPIV as light-in-flight holography (LiFH) by Hinrichs et al. (1997). Holography allows also more complex recording geometries incorporating stereoscopic viewing for evaluation of all components of the velocity vector and the possibility to store two or more holograms on one plate to provide for cross-correlation analysis (Herrmann 2000) or time series of particle holograms.

Nevertheless a constraint occurs in the size of the measuring volume due to the relatively slow photographic speed of holographic materials and the weakly scattering particles used in PIV. Even with powerful laser sources air flows have been investigated only in laboratory-scale experiments with dimensions of a few centimetres (Barnhart 1994, Pu and Meng 2000, Zhang et al. 1997).

## 2

### Holographic recording process: dynamic range, diffraction efficiency and image brightness

The common material used for recording high resolution holograms is a silver-halide film spin-coated on glass substrates, which can be developed in a negative process known from b/w-photography (reduction of silver-halide to silver atoms). Hence, a characteristic curve similar to b/w-films is found, showing amplitude transmission after development versus exposure (Fig. 1). Besides their high resolution (3000-5000 lp/mm) holographic films have a high dynamic range for recording intensity variations. The quality of a hologram is often measured by the proportion of reference light diffracted into the image during reconstruction. The best diffraction efficiency from a developed hologram is obtained using the full linear range, since then the recorded modulation serves as a sinusoidal grating with a maximized variation in the transmission characteristics. As shown in Fig. 1 the exposure is shifted by the reference intensity  $I_R$  towards the middle of the linear range and the object intensity  $I_O$  is used define the extent of the modulation. For common materials an object-to-reference ratio of  $r = I_O / I_R = 0.25$  is considered as a good starting point to produce holograms with high diffraction efficiency. The total exposure  $E = (I_O + I_R) \times t$  is controlled by varying the exposure time  $t$ . Decreasing  $r$  will result in loss of diffraction efficiency and hence lower image brightness when the holographic image is observed (e.g. by eye). When pulsed laser radiation is used to illuminate objects (e.g. particles in PIV) the exposure time  $t$  equals the pulse duration  $\tau$  and thus a minimum amount of object light per scattering particle is needed for proper recording. This obviously restricts the extent of the measuring volume, even more if a back scattering geometry is desired like in LiFH-PIV.

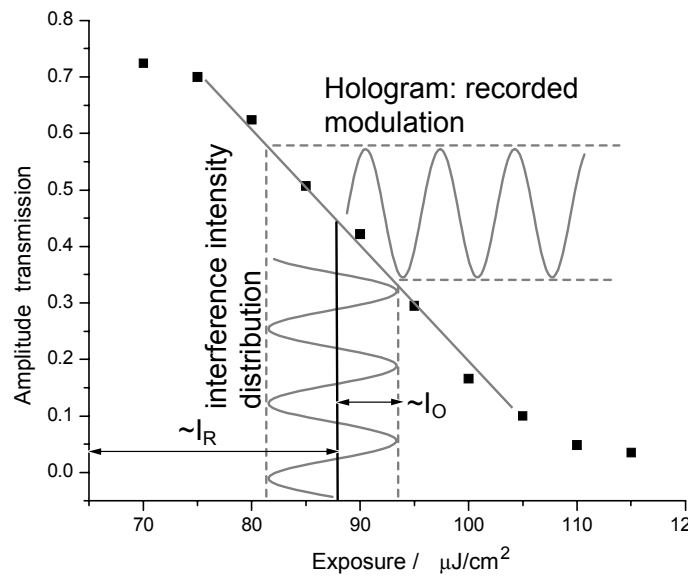


**Fig. 1 :** Characteristic  $T_a$ -E curve (amplitude transmission versus exposure) for the holographic emulsion Slavich PFG-01, the modulation transfer is depicted taking into account a ratio of object-to-reference intensity of  $r \approx 0.07$ .

### 3 Compensating the loss in diffraction efficiency

Using the real-image reconstruction provides a way to record the stored intensity distribution on photographic paper, film or a bare CCD sensor. This can be done for a volume slice by slice, a principle often used in HPIV setups. Using a continuous-wave laser this recording is not bound to fixed exposure times and hence a longer exposure time can be used to “collect” light even from a weakly diffracting hologram. The main limiting condition in such a time-averaging reconstruction process is the amount of scattered light from the emulsion grains and the diffuse external light reaching the medium. If the total amount (noise) is of the order of the diffracted light (signal) objects may vanish in a noisy background. The noise limit applicable to a common amplitude hologram is subject to this study, intended to find the lower bound on object light needed to record particle holograms.

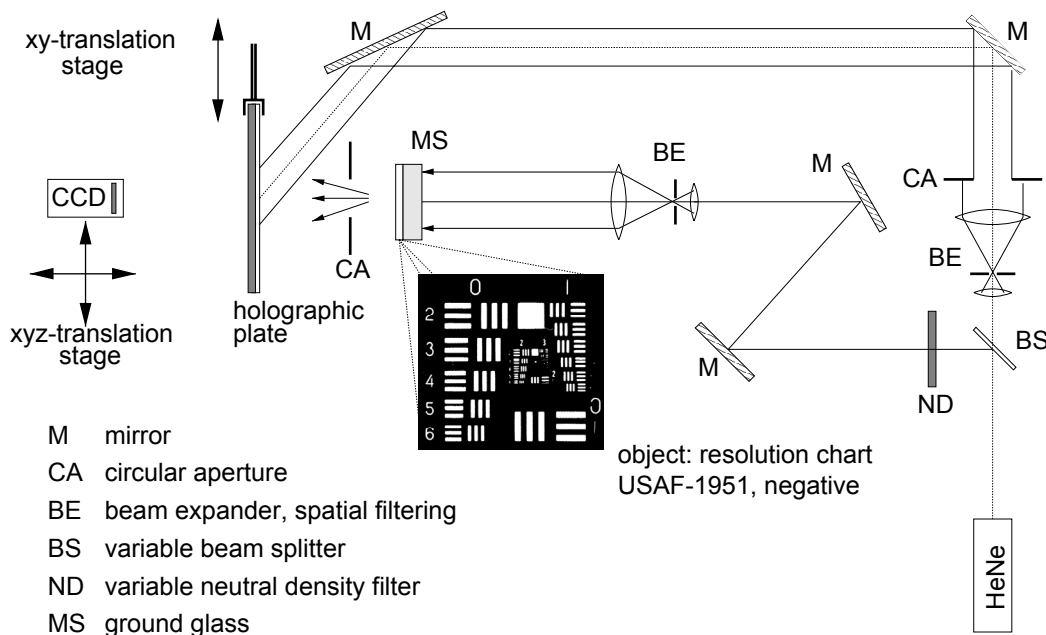


**Fig. 2:** Setup to record holograms of a test pattern with controlled object-to-reference intensity ratio, up to nine holograms could be recorded on one plate, the reconstruction of the virtual image is done in the same setup, a bare CCD sensor is used to digitize the image.

## 4

**The noise limit : influence of spatial frequency**

A first investigation of the noise limit was carried out with a test pattern known as resolution chart (USAF-1951 negative) providing a variety of spatial frequencies. An off-axis setup (Fig. 2) was used with a reference beam incident at  $45^\circ$  on the holographic plate to record and to reconstruct the test pattern. A ground glass directly adjacent to the glass substrate of the object produces light scattered towards the holographic plate from which only a small fraction was selected by a circular aperture to illuminate a limited part of the plate. The reference beam was also illuminating this part, producing elliptical holograms with axes of 33mm and 25mm, from which up to nine could be stored on one  $4'' \times 5''$  plate. It was thus possible to minimize fluctuations originating from the wet chemical processing within a series of holograms, developed all at once.

The total exposure was controlled by first adjusting the beam splitter to have an object-to-reference ratio of  $r = 0.25$  and then calculating the amount of reference light reaching the holographic plate. Therefore all losses due to the intermediate optics are taken into account. The exposure was set to a fixed value by controlling the exposure time of the following recordings to obtain a constant optical density throughout the experiment. By introducing neutral density filters in the object beam the amount of object light was reduced step by step.

After developing the plate was turned by  $180^\circ$  to reconstruct the real image using the same setup. This image was then digitized by a bare CCD sensor capable of long time exposure. The average gray level within a bright spot of the test pattern was kept constant using an adapted exposure time for the CCD. The effect of reduced  $r$  can be seen in Fig. 3. The superimposed speckle pattern becomes clearly visible when  $r > 10^{-4}$ .

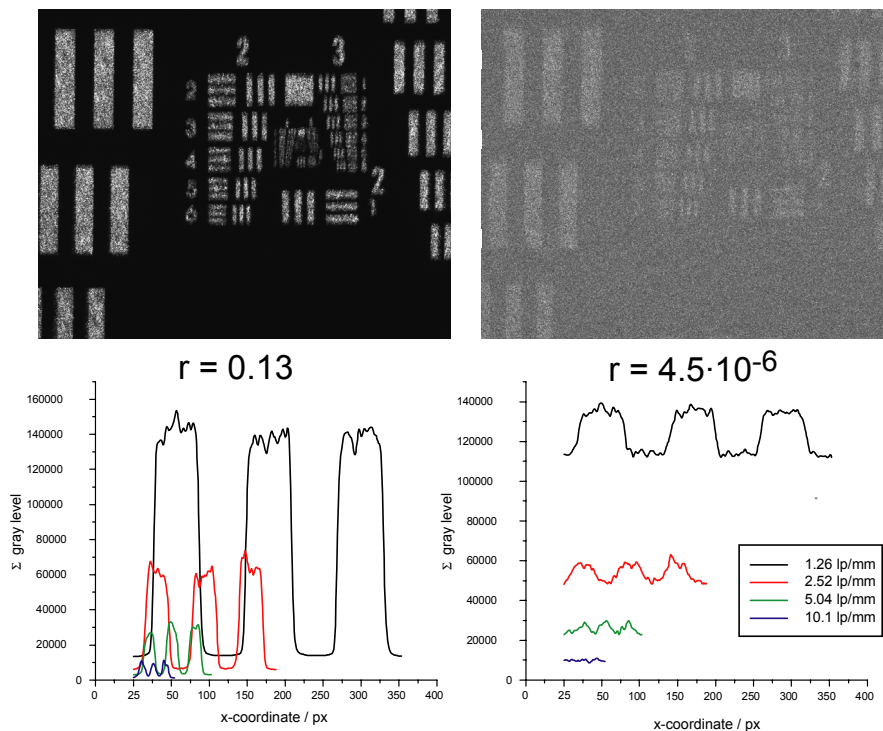


**Fig. 3:** Example reconstructions of the test pattern for two different ratios of the object-to-reference intensity  $r$  (top) and corresponding line-averaged profiles used to calculate the image visibility (bottom).

To study quantitatively the effect of reduced  $r$  the visibility  $V$  was calculated for each hologram and four spatial frequencies using image processing scripts under MATLAB<sup>®</sup>. First all scan-lines of each chosen vertical structure have been averaged to obtain a line-profile for the corresponding spatial frequency as depicted in Fig. 3. In a second step these profiles have been correlated with a rectangular function of the same spatial frequency to allocate the sections of the upper and lower level (Fig 4.). Then the values within each section are averaged to obtain  $G_{max}$  (upper level) and  $G_{min}$  (lower level) values from which the visibility  $V$  is calculated according to:

$$V = \frac{G_{max} - G_{min}}{G_{max} + G_{min}}. \quad (1)$$

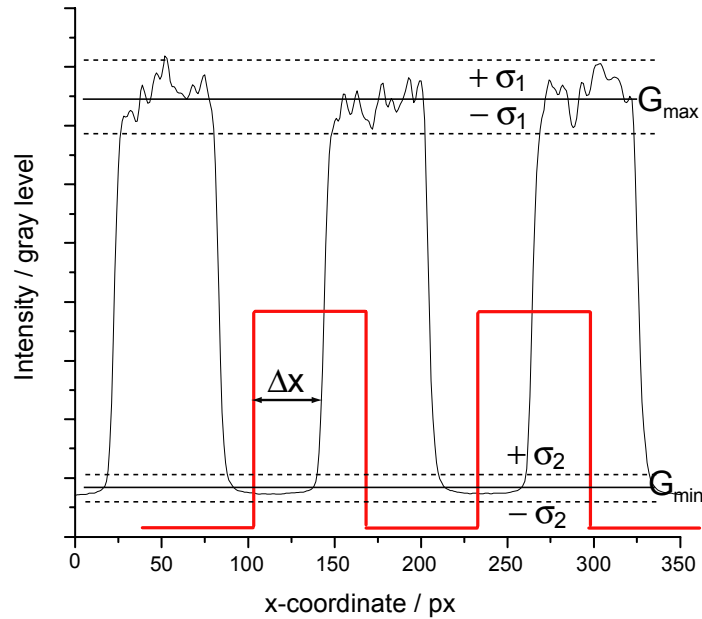


**Fig. 4:** Values within the profile are assigned to be either a max-value or a min-value by a correlation procedure to be averaged for the calculation of the visibility. A criterion to discard questionable values is formulated on the basis of the standard deviation of those values.

As a criterion for the acceptance of values of  $V$  the standard deviations  $\sigma_1$  and  $\sigma_2$  of both ranges are used to discard questionable results (Fig. 4). Values for the visibility  $V$  which comply with the following rule have been discarded:

$$G_{\max} - G_{\min} < \sigma_1 + \sigma_2. \quad (2)$$

Plotting the calculated visibility versus the ratio  $r$  of object-to-reference intensity (Fig. 5) shows distinct curves. Nevertheless, it is found that noise does not spoil the image quality for a range of approximately three orders of magnitude of  $r$ . A further decrease of  $r$  causes a constantly decreasing visibility. The fluctuations can be used to estimate the reproducibility of the wet chemical developing process. At certain values of  $r$  two holograms from different plates have been investigated, resulting in variations of the visibility of up to 20% at smaller values of  $r$ .

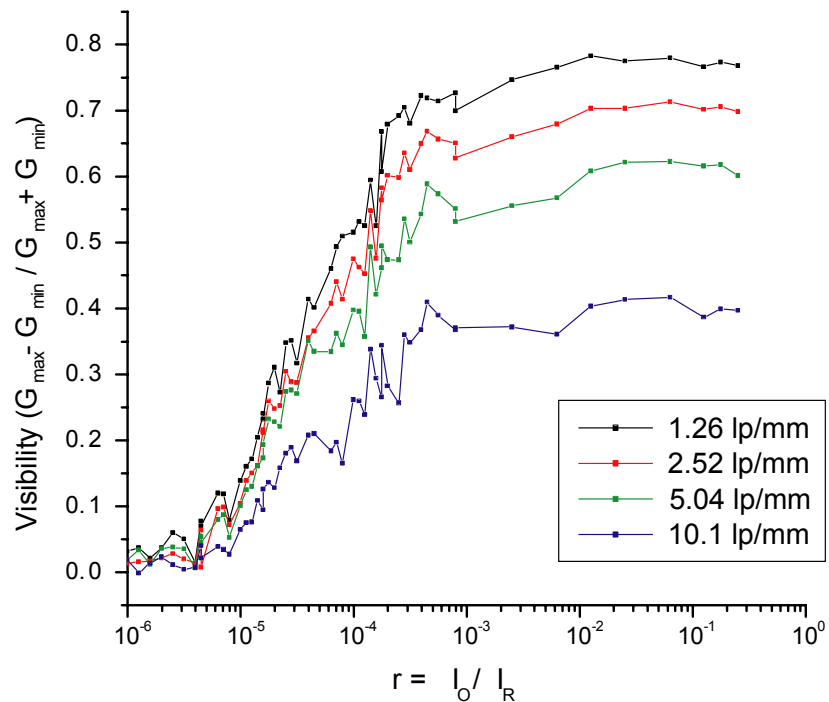


**Fig. 5:** Image visibility of the test pattern versus object-to-reference ratio  $r$  for four different spatial frequencies.

## 5

**HPIV: A model experiment**

In particle holography the investigated structural sizes are in general somewhat smaller and shapes are no more regular. It is therefore expected that signals vanish earlier in a noisy background when  $r$  is decreased. More realistically a PIV model experiment with a particle-laden block of PMMA was carried out to find the noise limit which prevents an evaluation by correlation techniques. Therefore the setup was modified to provide a thick light sheet (3mm) normal to the viewing direction and a translation stage to introduce a known displacement of the particle block (Fig. 6).

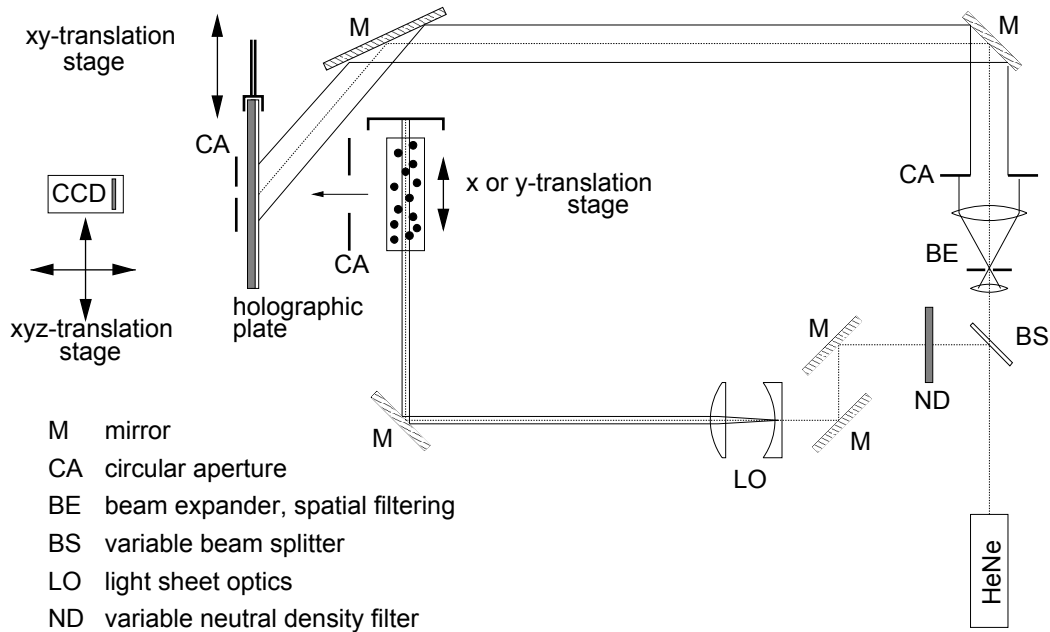


**Fig. 6:** Modified setup to provide for double exposed images for different values of the object-to-reference beam intensity ratio  $r$ . The particle block is illuminated with a light sheet normal to the viewing direction and translated between exposures to simulate HPIV recordings.

Each hologram was recorded using a double exposure and displacing the block in between. The reconstructed images ( $1280\text{px} \times 1024\text{px}$ ) have been evaluated using an autocorrelation algorithm giving more than 1000 individual interrogation areas of  $128\text{px} \times 128\text{px}$ . From each correlation function the corresponding SNR was used to characterize the image quality. According to Keane and Adrian (1990) we call this ratio detectability (Fig. 7):

$$D = R_d / R_n \quad (3)$$

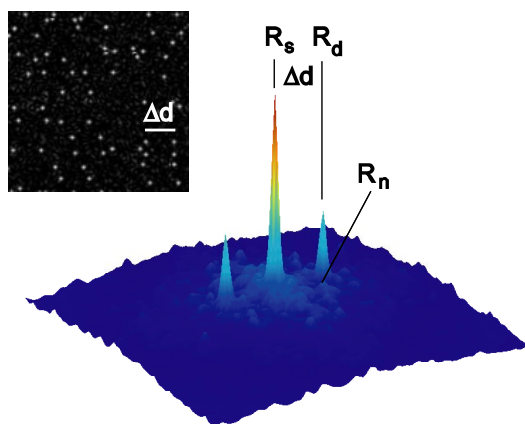


**Fig. 7:** The detectability  $D = R_d / R_n$  of particle pairs within an interrogation area is used to determine the image quality.

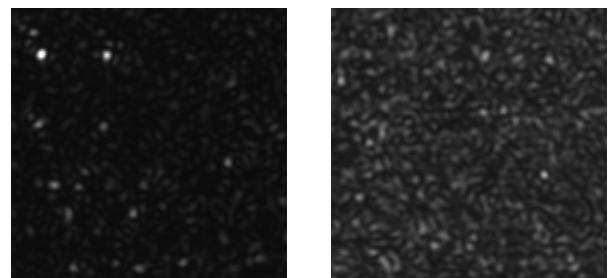


**Fig. 8:** Magnification of single interrogation areas ( $128\text{px} \times 128\text{px}$ ) from experiment with a model particle block at  $r = 3.1 \times 10^{-2}$  (left) and  $r = 1.5 \times 10^{-4}$  (right).

Samples of reconstructed images for different values of  $r$  are shown in Fig. 8, each giving a magnified view of one interrogation area. Even though the particle density is lower as recommended it becomes clear from inspecting the images that particle pairs tend to hide in a speckle pattern and thus their detectability is decreased. While the speckle size is similar to the size of the particle images the detectability becomes more and more independent of the number of particle pairs per interrogation area for decreasing  $r$  (i.e. brighter speckles). This is due to the self correlation of the speckle field which produces numerous peaks  $R_n$  similar in size to  $R_d$ .

An estimate of the noise limit in particle holography is obtained by plotting the detectability  $D$  versus the object-to-reference intensity ratio  $r$  as shown in Fig. 9. In this plot the detectability for each hologram is an average value of the detectability of all interrogation areas in one image. The influence of variations of particle density and brightness is thus minimized. However, it can be found from Fig. 9 that reproducibility is a crucial point in this experiment and only tendencies can be extracted from the data. The noise limit for this kind of image processing (evaluation by autocorrelation) is found at a beam ratio of  $r \approx 10^{-3}$ . Presuming that only small fractions of light are scattered by particles contained in an illuminated volume (i.e. constant energy density throughout a given beam profile) the cross section of the illumination can thus be increased by a factor of 25. Typical HPIV experiments with present length scales in the order of 100 mm could thus be extended to dimensions of 500 mm.

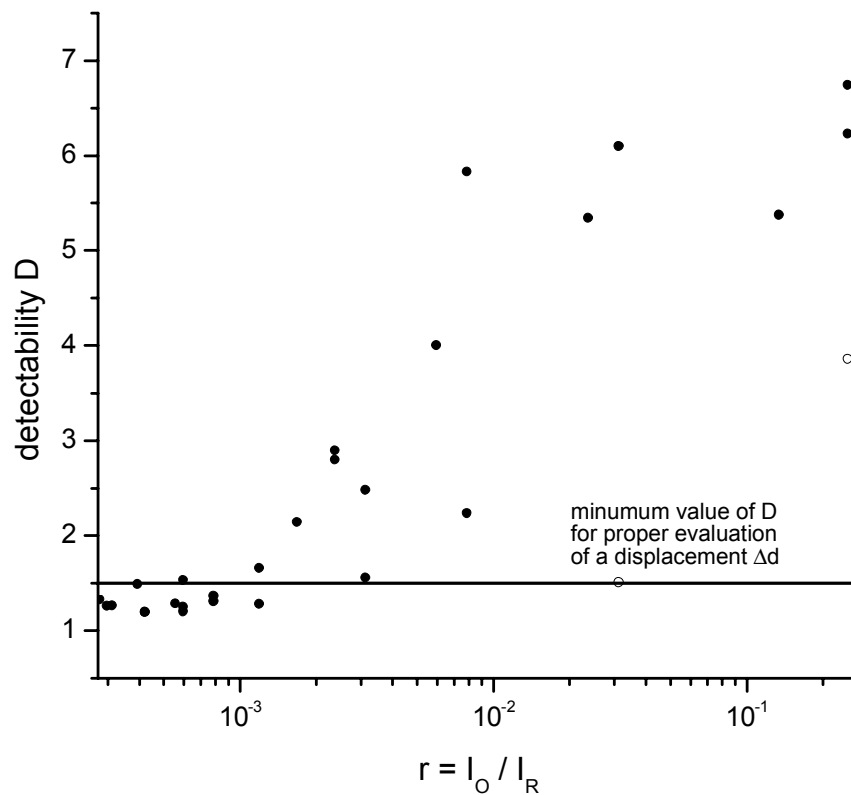


**Fig. 9:** Experimental data on the influence of a decreasing object-to-reference intensity ratio  $r$  during the recording of a double-exposed particle hologram. The detectability  $D$ , a measure to detect a displacement of particles introduced between the two exposures, is shown versus  $r$ .

## 6

### Theoretical description of light scattered by emulsion grains

To describe the influence of light scattering by grains in an emulsion a model based on a checkerboard like distribution of grains is assumed. A theory developed by Goodman, Kozma and Friesem (1967) predicts a linear relationship between the SNR in a point-like image and the object-to-reference beam intensity ratio  $r = I_O / I_R$ . The SNR herein is given by the ratio of the image intensity  $I_i$  and the statistical average of the speckle intensities  $\langle I_n \rangle$  in the background:

$$\frac{I_i}{\langle I_n \rangle} = \frac{K^2 \eta^2 A_t}{\phi(v)} \cdot r \quad (4)$$

The slope in this relation is given by a factor composed of properties of the hologram, namely a factor  $K$  depending on the modulation transfer function of the holographic material, the slope  $\eta$  of its characteristic curve (normalized  $T_a$ -E curve), the area  $A_t$  of the hologram and the Wiener spectrum  $\phi(\nu)$  of the noise (i.e. the power of light scattered into a certain spatial frequency divided by the power incident on the hologram). The primary spatial frequency  $\nu$  is given by the angle between object and reference beam.

A good agreement between this theory and an experiment was obtained by Meng and Hussain (1995), who have used a pinhole as a point-like object. Using a beam ratio of  $r = 10^{-8}$  for recording the hologram it was possible to distinguish the reconstructed single point from the background. Substituting the values  $\nu=300$  lp/mm,  $\phi(\nu) = 0.47 \times 10^{-8}$ ,  $K = 0.95$ ,  $\eta = 0.56$  and  $A_t = 100\text{mm}^2$  for Kodak 694F plates in (4) and assuming an SNR of 50 the corresponding minimum beam ratio would be  $r = 0.83 \times 10^{-8}$ .

Now let us assume a particle field consisting of  $N$  particles which is recorded in such a way, that each particle is resolved in the reconstructed image. Then the amount of object light  $I_{\Sigma O}$  is the sum of light  $I_O$  scattered by each particle, and we obtain a new beam ratio  $r$ :

$$r = \frac{I_{\Sigma O}}{I_R}, \text{ with } I_{\Sigma O} = N \cdot I_O. \quad (5)$$

Hence the minimum beam ratio also depends on  $N$  and equation (4) has to be rewritten:

$$\frac{I_i}{\langle I_n \rangle} = \frac{K^2 \eta^2 A_t}{\phi(\nu) \cdot N} \cdot r. \quad (6)$$

The SNR of the images under investigation is closely related to the detectability in a correlation scheme to evaluate displacements. A Monte-Carlo simulation was used to explore the influence of speckle size and SNR on the detectability using an autocorrelation algorithm (Fig. 10). Smaller speckle sizes permit slightly lower SNR to reach a certain detectability, while around  $\text{SNR} = 100$  the influence of the speckle field is no longer observed.

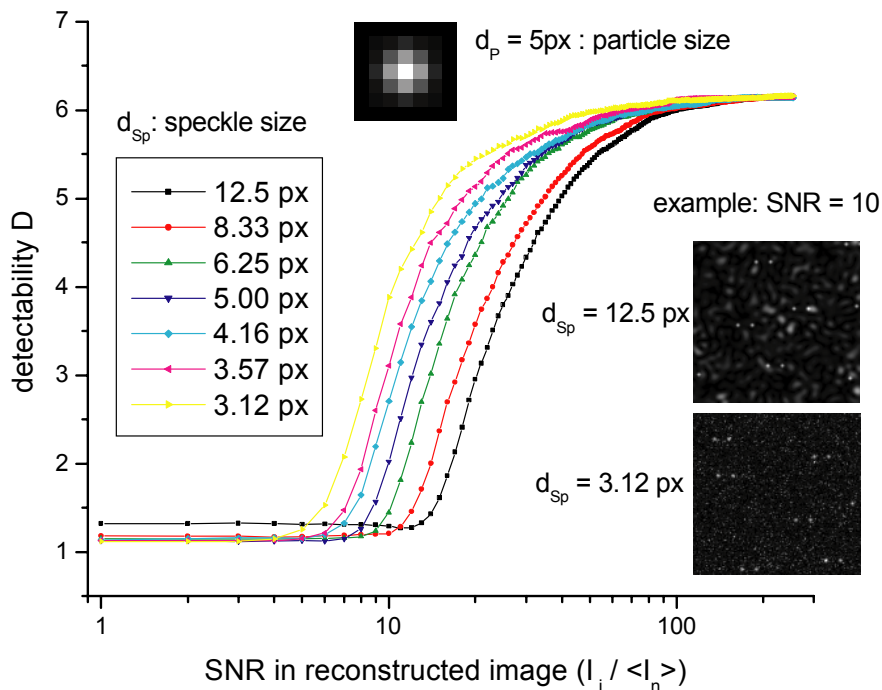


**Fig. 10:** Monte-Carlo simulation to describe the influence of speckle size and SNR in particle images on the detectability using auto correlation algorithms.

To check our experimental data the theory described above is adapted to fit the properties of the holographic material which has been used and the characteristics of our experiment. For a given SNR obtained from the simulation the corresponding beam intensity ratio  $r$  can be calculated using equation (6) and substituting the following values:  $\phi(\nu) = 1 \times 10^{-8}$ ,  $K = 0.87$ ,  $\eta = 0.526$ ,  $A_t = 20\text{mm}^2$  and  $N = 3.3 \times 10^4$ . It has to be mentioned that the

value for the Wiener spectrum is only a rough estimation and has yet not been measured for the Slavich PFG-01 plates. The resulting behavior shown in Fig. 11 slightly underestimates the measured data.

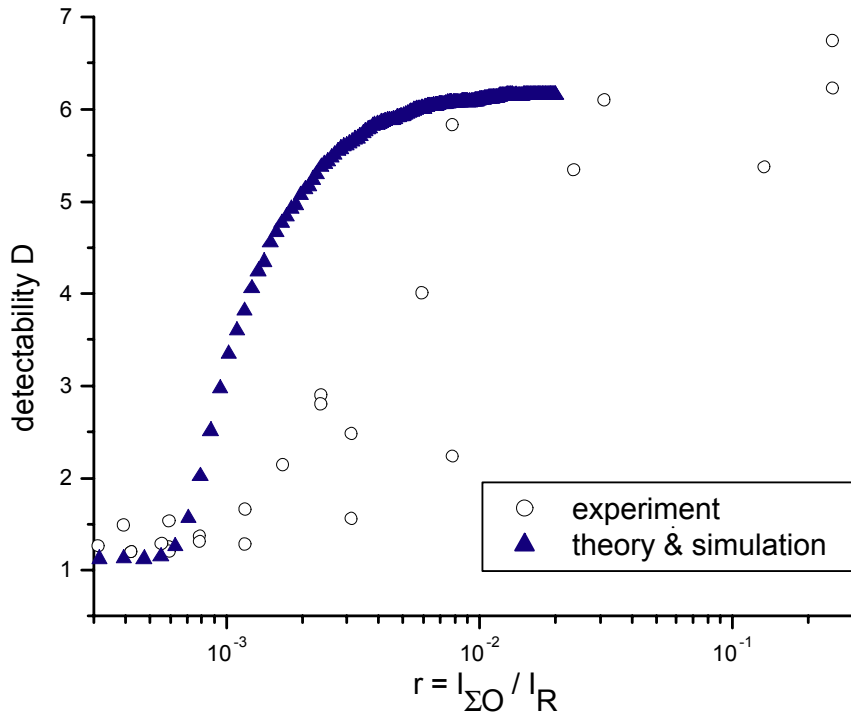


**Fig. 11:** Theoretical behaviour of detectability  $D$  versus beam intensity ratio  $r$  for Slavich PFG-01 plates. The experimental data obtained with these plates is shown for the purpose of comparison.

## 7

### Conclusions

In HPIV present restrictions in the size of the volume under investigation can be relaxed by taking advantage of the high dynamic range of common holographic materials. For less object light than needed to produce bright holographic images a method has been proposed using a time-integrating reconstruction. This principle can be used to compensate for the loss in diffraction efficiency. Limits of this technique are given by disturbing background light, mainly scattered from the silver grains in the developed holographic emulsion. It has been shown that considerable reductions of object light are tolerable, still enabling the reconstruction of object images. General experiments on test targets give a first idea about the limits of this technique. For particle holography these limits are strongly related to the number of particles, as also shown in a theoretical approach. Nevertheless, for common HPIV setups a considerable gain in the dimensions of the measuring volume is expected. Thus, applications in larger flow facilities become feasible.

### Acknowledgements

The authors would like to thank H. Sroka and M. Ohm for her eminent work at the experiments with the test target. The valuable contributions of P. Arroyo, H. Helmers and T. Fricke-Begemann discussing the topic are greatly appreciated. This work was partially funded by financial support of the EC (EUROPIV2: G4RD-CT-2000-00190).



## References

- Barnhart DH; Adrian RJ; Papen GC** (1994) Phase conjugate holographic system for high resolution particle image velocimetry, *Applied Optics* **33**, pp.7159-7170
- Friesem AA; Kozma A; Adams G** (1967) Recording parameters of spatial modulated coherent wavefronts, *Applied Optics* **6(5)**, pp.851-856
- Goodman JW** (1967) Film grain noise in wavefront-reconstruction imaging, *JOSA* **57(4)**, pp. 493-502
- Herrmann SH; Geiger M; Hinsch KD; Peinke J** (2000) Light-in-flight holography with switched reference beams for cross-correlation in deep volume PIV, Proc. 10<sup>th</sup> Intern. Symp. on Applications of Laser Techniques to Fluid Mechanics, Lisbon, Portugal, July 2000, paper 2.1
- Kean RD; Adrian RJ** (1990) Optimization of particle image velocimeters. Part I: Double pulsed systems, *Meas.Sci.Technol.* **1**, pp.1202-1215
- Kozma A** (1967) Effects of film-grain noise in holography, *JOSA* **58**, pp.436-438
- Meng H; Hussain F** (1995) In-line recording and off-axis viewing technique for holographic particle velocimetry, *Applied Optics* **34**, pp.1827-1840